

## Field Profile of Asymmetric Slab Waveguide Structure with LHM Layers

S.A. Taya\*, Kh.Y. Elwasife†

Physics Department, Islamic University of Gaza, Palestinian Authority

(Received 16 March 2014; published online 20 June 2014)

This paper presents asymmetric three-layer slab waveguide structure in which all layers are considered left-handed materials (LHMs) with negative electric permittivity and magnetic permeability. The electric field profile is investigated in details with all parameters of the waveguide structure. Many interesting features are observed such as the existence of the fundamental mode and the transition from the fundamental mode to the first guided mode with increasing the imaginary part of the guiding layer permittivity or permeability.

**Keywords:** Slab waveguides, Guided modes, Left-handed materials.

PACS numbers: 42.65.Wi, 42.65.Tg, 42.25.Bs

### 1. INTRODUCTION

Several groups have succeeded in fabricating left-handed media and it is now possible to employ left-handed electromagnetism in a large range. In recent years, the topic of metamaterials, i.e. artificial materials synthesized by embedding specific inclusions in host media, has increasingly received a renewed attention due to the interest in man-made complex materials that may possess negative permittivity ( $\epsilon$ ) and permeability ( $\mu$ ) in a certain frequency band. In 1968, Veselago postulated theoretically a material in which both  $\epsilon$  and  $\mu$  were assumed to have negative real values and he analyzed plane wave propagation in such a medium [1]. These materials were called left-handed metamaterials (LHMs). Since then an intensive research has been carried out to understand the properties of electromagnetic waves in these media [2-20]. I. V. Shadrivov analyzed nonlinear guided waves in a planar waveguide made of a LHM surrounded by a Kerr-like nonlinear dielectric and predicted that such a waveguide can support fast and slow symmetric and antisymmetric nonlinear modes [2]. Moreover, he studied the symmetry breaking bifurcation and asymmetric modes in such a symmetric structure and showed that the modes can be either forward or backward [2]. Characteristics of surface wave modes on a grounded slab of LHM were investigated [3]. It was shown that, unlike a slab with positive parameters, the dominant mode can have evanescent fields on both sides of the interface between the slab and the surrounding air. The guided and surface modes in an LHM asymmetric slab waveguide were studied by introducing three normalized parameters [4-8]. The guided dispersion characteristics of the fundamental symmetric and asymmetric modes of surface waves along single- and double-negative indexed slab waveguides were investigated and a comparative analysis was made when varying the single- and double-negative permittivity and permeability [9]. Asymmetric waveguide structure with a LHM guiding layer surrounded by a linear dielectric substrate and a gyromagnetic ferrite cladding has been investigated [10]. Guided modes supported by an asymmetric three-layer metal-clad waveguide structure were presented when the

guiding layer is LHM [11]. Multilayer planar waveguide structures comprising LHMs have been explored for both TM and TE polarizations [12-14]. TE surface modes guided by a single interface and a slab waveguide containing LHMs were analyzed by using a ray picture [15]. The transfer function of the discretized perfect lens in finite-difference time-domain and transfer matrix method simulations was investigated [16]. Waveguide structures comprising LHMs have been strong candidates for many optoelectronics applications. One of the most interesting applications of LHM waveguide structures is optical sensing [17-20] in which any change in the refractive index of the analyte is detected.

In this paper asymmetric three-layer planar waveguide structure is studied for both TE and TM modes. All layers are considered to be LHMs. The field profile is investigated in details with all parameters of the LHMs.

### 2. THEORY

We suppose an asymmetric three-layer slab waveguide structure. The substrate, guiding film, and cladding are assumed to be LHMs with  $\epsilon_i < 0$  and  $\mu_i < 0$  ( $i = 1, 2, 3$ ). The waves are considered to propagate along  $z$ -direction and  $x$ -axis is perpendicular to the plane separating the structure layers as shown in Fig. 1.

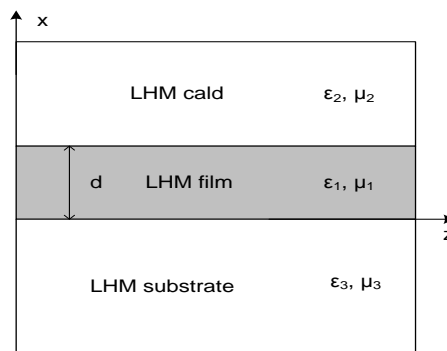


Fig. 1 – Cross-sectional view of asymmetric LHM slab waveguide

\* staya@iugaza.edu.ps

† kelwasife@iugaza.edu.ps

Since the waveguide is homogeneous along  $z$ -axis, solutions to the wave equation can have the form

$$\vec{E}(x, z, t) = E_y(x) \exp(j(\omega t - \beta z)) \hat{a}_y, \quad (1)$$

$$\vec{H}(x, z, t) = [H_x(x) \hat{a}_x + H_z(x) \hat{a}_z] \exp(j(\omega t - \beta z)), \quad (2)$$

where  $\omega$  is the angular frequency and  $\beta$  is the propagation constant. The wave vector components  $h$ ,  $q_2$ , and  $q_3$  are defined as  $h = \sqrt{k_0^2 \varepsilon_1 \mu_1 - \beta^2}$ ,  $q_2 = \sqrt{\beta^2 - k_0^2 \varepsilon_2 \mu_2}$ ,  $q_3 = \sqrt{\beta^2 - k_0^2 \varepsilon_3 \mu_3}$ .

The  $y$ -component of the electric field for TE polarization is given by

$$E_y(x) = \begin{cases} (A \sin(hx) + B \cos(hx)) & 0 < x < d \\ C \exp(-q_2 x) & x > d \\ D \exp(q_2 x) & x < 0 \end{cases} \quad (3)$$

The magnetic field is given by

$$\vec{H} = \frac{\nabla \times \vec{E}}{-j\omega\mu}, \quad (4)$$

resulting in

$$H_z(x) = \frac{j}{\omega\mu} \frac{\partial E_y}{\partial x} \quad (5)$$

The boundary conditions require that the tangential components of both  $\vec{E}$  and  $\vec{H}$  are continuous across the boundaries. The boundary condition equation for the asymmetric modes is given by

$$\tan(hd) = \frac{\frac{\mu_1 q_3}{\mu_3 h} + \frac{\mu_1 q_2}{\mu_2 h}}{1 - \frac{\mu_1 q_3}{\mu_3 h} \frac{\mu_1 q_2}{\mu_2 h}} \quad (6)$$

To introduce the mode order ( $m$ ), Eq. (6) can be written as

$$hd = \tan^{-1} \left( \frac{\mu_1 q_3}{\mu_3 h} \right) + \tan^{-1} \left( \frac{\mu_1 q_2}{\mu_2 h} \right) + m\pi. \quad (7)$$

The right-hand side (RHS) of Eq. (6) can be written as a function of  $(hd)$ . We first assume  $q_2$  and  $q_3$  to have the forms

$$q_2 = \sqrt{k_0^2 (\varepsilon_1 \mu_1 - \varepsilon_2 \mu_2) - h^2}, \quad (8)$$

$$q_3 = \sqrt{k_0^2 (\varepsilon_1 \mu_1 - \varepsilon_3 \mu_3) - h^2} \quad (9)$$

with these notation for  $q_1$  and  $q_3$ , the RHS of Eq. (6) can be written as

$$F(hd) = hd \frac{\frac{\mu_2}{\mu_1} \sqrt{s^2 - (hd)^2} + \frac{\mu_3}{\mu_1} \sqrt{p^2 - (hd)^2}}{(hd)^2 \frac{\mu_2 \mu_3}{\mu_1^2} - \sqrt{s^2 - (hd)^2} \sqrt{p^2 - (hd)^2}} \quad (10)$$

where  $s = k_0 d \sqrt{\varepsilon_1 \mu_1 - \varepsilon_2 \mu_2}$  and  $p = k_0 d \sqrt{\varepsilon_1 \mu_1 - \varepsilon_3 \mu_3}$ .

When propagation constant  $\beta$  exceeds a critical value, the wave number  $h$  becomes purely imaginary.

For TM polarization, the boundary condition equation is given by

$$\tan(hd) = \frac{\frac{\varepsilon_1 q_3}{\varepsilon_3 h} + \frac{\varepsilon_1 q_2}{\varepsilon_2 h}}{1 - \frac{\varepsilon_1 q_3}{\varepsilon_3 h} \frac{\varepsilon_1 q_2}{\varepsilon_2 h}} \quad (11)$$

### 3. RESULTS AND DISCUSSION

Figure 1 shows the slab waveguide geometry under consideration. In the analysis below, the frequency of electromagnetic waves is assumed to be 4.6GHz. Oscillating mode can exist in the proposed structure for  $k_0^2 \varepsilon_1 \mu_1 > \beta^2 > k_0^2 \varepsilon_3 \mu_3$ . Graphical method can be used to determine the values of  $hd$  for possible guided modes.  $\tan(hd)$  given by Eq. (6) and  $F(hd)$  given by Eq.(10) are plotted versus  $hd$  in Fig. 2. The intersection points give the values of  $hd$  at which the guided modes exist. It is clear from the figure that the proposed structure can support guided modes. Transverse profiles of the TE<sub>0</sub> mode for different values of the operating frequency are plotted in Fig. 3 for  $\mu_s = \mu_f = \mu_c = -1 + 0.001i$ ,  $\varepsilon_s = -4.7 + 0.001i$ ,  $\varepsilon_f = -5.7 + 0.001i$ , and  $\varepsilon_c = -3.7 + 0.001i$ . The guiding layer thickness is assumed to be 6  $\mu\text{m}$ . As can be seen from the figure, the electric field oscillates in the guiding layer and is evanescent in the surrounding media. The two tails of the evanescent are asymmetric in the substrate and cladding due to the asymmetric structure assumed. Increasing the angular frequency of the guided wave from 4.6 GHz to 5 GHz does not have a considerable effect on the field profile. It merely enhances the peak of the oscillating waves in the guiding layer. Moreover, it causes a barely detectable reduction in the evanescent field in the surrounding media. It is worth to mention that the waveguide structure considered in this work can accommodate the fundamental mode. The absence of the fundamental mode was reported in many works in literature [7] when a LHM guiding layer is surrounded by two linear dielectric media. Our investigation here of a LHM guiding layer surrounded by two LHMs emphasizes that this structure can support any mode including the fundamental one. Transverse profiles of the fundamental mode for different values of the permittivity (left) and permeability (right) of the film are shown in Fig. 4. As can be seen from the figure, increasing the absolute value of  $\text{Re}(\varepsilon_f)$  or  $\text{Re}(\mu_f)$  reduces the evanescent field in the substrate and cladding layers. Moreover, it leads to an enhancement of the oscillating wave peak in the guiding layer. This property is very similar to that of conventional guided modes in the well-known dielectric waveguides in which the increasing of the guiding layer refractive index enhances the confinement of the wave and reduces the wave tails in the surrounding media. The distributions of electric field amplitude in the waveguide for different values of the substrate permittivity (left) and permeability (right) are shown in Fig. 5. The most important feature that can be ob-

served from the figure is the shift of the field profile towards the substrate layer as the absolute value of  $\text{Re}(\epsilon_s)$  or  $\text{Re}(\mu_s)$  increases. Figure 6 shows the same behavior as that observed in Fig. 5, but with the cladding parameters. The field peak moves towards the film-cladding interface as the absolute value of  $\text{Re}(\epsilon_c)$  or  $\text{Re}(\mu_c)$  increases leading to the enhancement of the evanescent field in the cladding layer. This enhancement is of great benefit for optical waveguide sensor applications [17-19]. We now turn our attention to the effect of imaginary parts of  $\epsilon$  and  $\mu$  of the three layers constituting the waveguide structure under consideration. The imaginary parts of  $\epsilon$  and  $\mu$  are of great significance in LHMs since lossless LHMs are not realistic. The electric field distribution in the waveguide is shown in Fig. 7 for different values of  $\text{Im}(\epsilon_f)$ . The mode order ( $m$ ) in Eq. (7) represents the number of intersections between the field curve and the  $x$ -axis in the guiding layer region. When the field curve does not intersect the  $x$ -axis in the guiding layer, the fundamental mode exists. As the figure shows, for  $\text{Im}(\epsilon_f) = 0.01, 0.05, \text{ and } 0.1$ , the guided mode is the fundamental one. There is a transition from the fundamental mode ( $\text{TE}_0$ ) to the first mode ( $\text{TE}_1$ ) as the  $\text{Im}(\epsilon_f)$  increases to 0.15 and 0.20. This is a significant feature showing the importance of the imaginary part of  $\epsilon_f$ . As the  $\text{Im}(\epsilon_f)$  increases, an additional phase shift is imposed on the guided wave. This phase condition changes the fundamental mode ( $m = 0$ ) to the first mode  $m = 1$ . Figure 8 shows the same behavior when increasing the imaginary part of  $\mu_f$ . The fundamental mode profile in the film layer shifts to the next mode when the  $\text{Im}(\mu_f)$  exceeds a specific value.

The electric field distribution of guided modes  $\text{TE}_0, \text{TE}_1, \text{TE}_2,$  and  $\text{TE}_3$  are illustrated in Fig. 9. Their properties are very similar to those of conventional guided modes in normal dielectric waveguides. In all these modes, the electric field is oscillatory in the guiding layer and evanescent in the substrate and cladding layers. As mentioned before, the number of intersections between the field curve and the  $x$ -axis in the film layer is equal to the mode order. The figure also shows that the transverse distribution peaks are asymmetric because of asymmetric structure assumed.

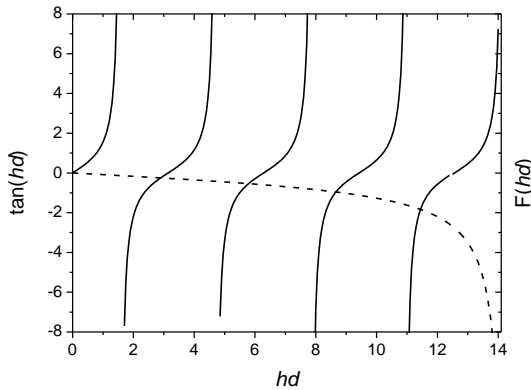


Fig. 2 – Graphical determination of  $hd$  for oscillating guided modes of an asymmetric LHM waveguide

Finally, we investigate the properties of p-polarized light. Figure 10 depicts the transverse field profiles of the fundamental modes  $\text{TE}_0$  and  $\text{TM}_0$ . No remarkable differences can be found between the two polarizations. The field is oscillatory in the film layer while it becomes evanescent in the surrounding media. A little enhancement is observed in the field peak for  $\text{TM}_0$  mode.

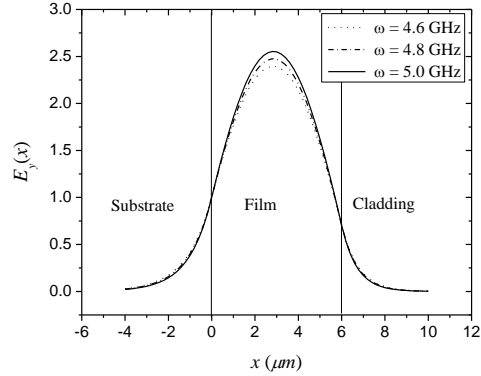


Fig. 3 – Transverse profiles of the fundamental mode ( $\text{TE}_0$ ) for different values of the operating frequency for  $\mu_s = \mu_f = \mu_c = -1 + 0.001i$ ,  $\epsilon_s = -4.7 + 0.001i$ ,  $\epsilon_f = -5.7 + 0.001i$ , and  $\epsilon_c = -3.7 + 0.001i$

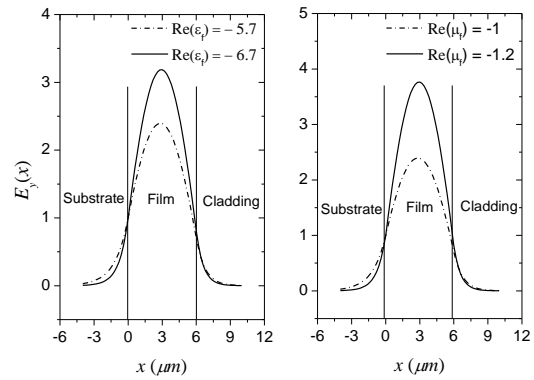


Fig. 4 – Transverse profiles of the fundamental mode ( $\text{TE}_0$ ) for different values of the permittivity (left) and permeability (right) of the film for  $\mu_s = \mu_c = -1 + 0.001i$ ,  $\epsilon_s = -4.7 + 0.001i$  and  $\epsilon_c = -3.7 + 0.001i$

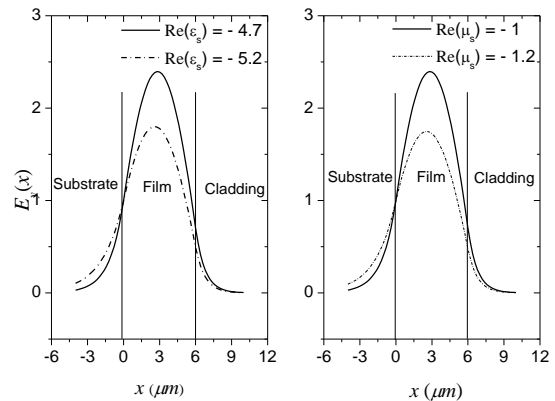
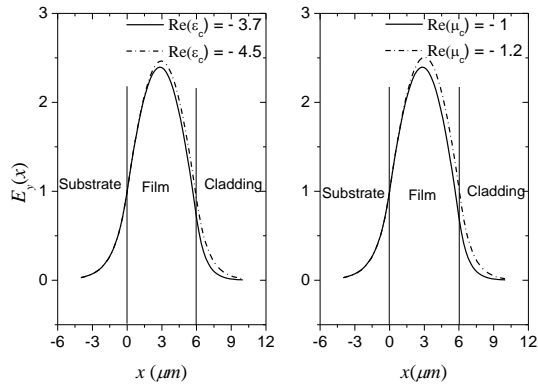
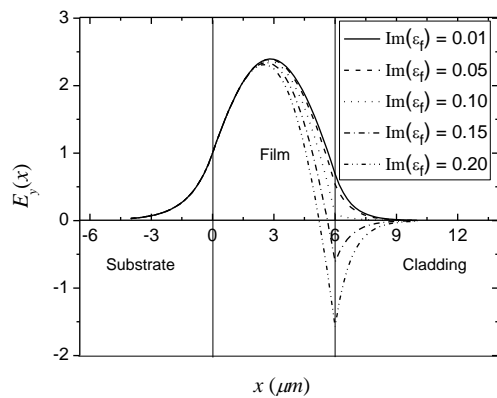


Fig. 5 – Transverse profiles of the fundamental mode ( $\text{TE}_0$ ) for different values of the permittivity (Left) and permeability (right) of the substrate for  $\mu_f = \mu_c = -1 + 0.001i$ ,  $\epsilon_f = -5.7 + 0.001i$ , and  $\epsilon_c = -3.7 + 0.001i$



**Fig. 6** – Transverse profiles of the fundamental mode (TE<sub>0</sub>) for different values of the permittivity (left) and permeability (right) of the cladding for  $\mu_s = \mu_f = \mu_c = -1 + 0.001i$ ,  $\varepsilon_f = -5.7 + 0.001i$ , and  $\varepsilon_s = -4.7 + 0.001i$



**Fig. 7** – Transverse profiles of the fundamental mode (TE<sub>0</sub>) for different values of the imaginary part of  $\varepsilon_f$  for  $\omega = 4.6$  GHz,  $\mu_s = \mu_f = \mu_c = -1 + 0.001i$ ,  $\varepsilon_s = -4.7 + 0.001i$ , and  $\varepsilon_c = -3.7 + 0.001i$

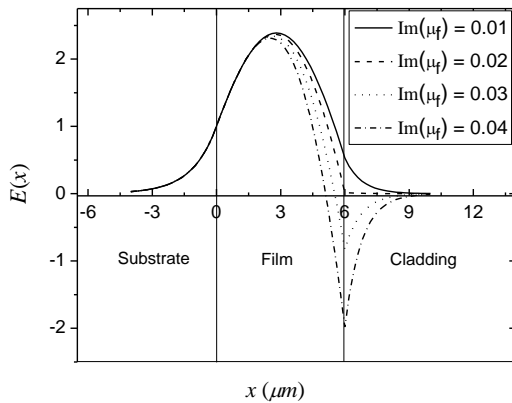


**Fig. 8** – Transverse profiles of the fundamental mode (TE<sub>0</sub>) for different values of the imaginary part of  $\mu_f$  for  $\omega = 4.6$  GHz,  $\mu_s = \mu_c = -1 + 0.001i$ ,  $\varepsilon_s = -4.7 + 0.001i$ ,  $\varepsilon_f = -5.7 + 0.001i$  and  $\varepsilon_c = -3.7 + 0.001i$

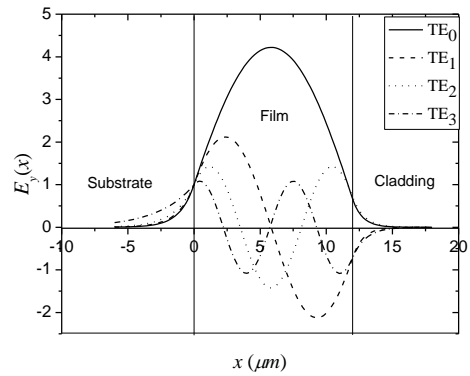


**Fig. 9** – Transverse profiles of different mode (TE) orders for  $\omega = 4.6$  GHz,  $\mu_s = \mu_f = \mu_c = -1 + 0.001i$ ,  $\varepsilon_s = -4.7 + 0.001i$ ,  $\varepsilon_f = -5.7 + 0.001i$ , and  $\varepsilon_c = -3.7 + 0.001i$

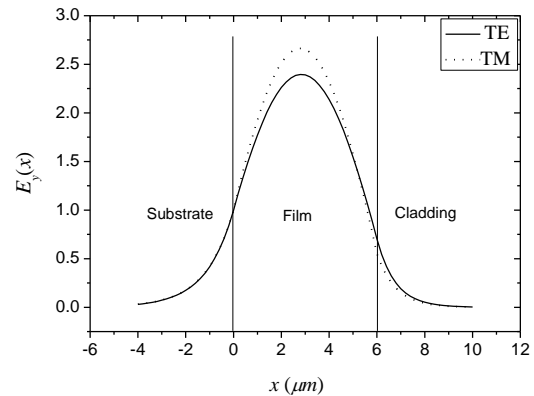


**Fig. 10** – Transverse profiles of TE<sub>0</sub> and TM<sub>0</sub> polarizations for  $\omega = 4.6$  GHz,  $\mu_s = \mu_f = \mu_c = -1 + 0.001i$ ,  $\varepsilon_s = -4.7 + 0.001i$ ,  $\varepsilon_f = -5.7 + 0.001i$ , and  $\varepsilon_c = -3.7 + 0.001i$

**4. CONCLUSION**

Asymmetric three-layer slab waveguide structure was considered. All layers were assumed to have a negative index of refraction. The propagation of electromagnetic waves in such a structure was treated. It was found that the structure can support guided modes of any order. The fundamental mode can exist as well as higher modes. Moreover, it was found that increasing the imaginary part of the guiding layer permittivity or permeability change the fundamental mode to the first mode.

**REFERENCES**

1. V.G. Veselago, *Sov. Phys.* **10** No 4, 509 (1968).
2. Ilya V. Shadrivov, *Photonics and Nanostructures – Fundamentals and Applications* **2**,175 (2004).
3. S. Mahmoud, A.J. Viitanen, *Prog. Electromagnetic Res.* **51**, 127 (2005).
4. Z.J. Wang, J.F. Dong, *Prog. Electromagnetics Res.* **62**, 203 (2006).
5. S.A. Taya, I.M. Qadoura, *Optik- Int. J. Light Electron Opt.* **124** No 13, 1431 (2012).
6. I.M. Qadoura, S.A. Taya, K.Y. El-Wasife *IJMOT* **7** No 5, 349 (2012).
7. S.A. Taya, H.M. Kullab, I.M. Qadoura, *J. Opt. Soc. Am. B* **30** No 7, 2008 (2013).
8. Z.H. Wang, Z.Y. Xiao, S.P. Li, *Opt. Commun.* **281**, 607 (2008).

9. K.Y. Kim, Y.K. Cho, *Opto-Electron. Rev.* **18**, 388 (2010).
10. Kh.Y. El-Wasife, S.A. Taya, *Instanci J. Phys.* **1** No1, 21 (2011).
11. S.A. Taya, Kh.Y. Elwasife, *Int. J. Res. Rev. Appl. Sci.* **13**, No 1, 294 (2012).
12. S.A. Taya, E.J. El-Farram, M.M. Abadla, *Optik* **123**, No 24, 2264 (2012).
13. M.A. Abadla, S.A. Taya, *The Islamic University Journal* **19** No 1, 57 (2011).
14. H.M. Kullab, S.A. Taya, *Int. J. Electron. Commun. (AEÜ)* **67** No 11, 905 (2013).
15. Zi. Hua Wang, Su. Ping Li, *J. Opt. Soc. Am. B* **25** No 6, 903 (2008).
16. Th. Koschny, R. Moussa, C.M. Soukoulis, *J. Opt. Soc. Am. B* **23**, No 3, 485 (2006).
17. H.M. Kullab, S.A. Taya, *Int. J. Light Electron Opt.* **145** No 1, 97 (2014).
18. S.A. Taya, H.M. Kullab, *Appl. Phys. A* (2014) [in Press].
19. H.M. Kullab, S.A. Taya, T.M. El-Agez, *J. Opt. Soc. Am. B* **29**, 959 (2012).
20. M. Abadla, S.A. Taya, *Int. J. Light Electron Opt.* **125**, No 3, 1401 (2014).